

# NUCLEOSIDE PHOSPHATASE AND CHOLINESTERASE ACTIVITIES IN DORSAL ROOT GANGLIA AND PERIPHERAL NERVE

ALEX B. NOVIKOFF, NELSON QUINTANA, HUMBERTO  
VILLAYERDE, and REGINA FORSCHIRM

From the Department of Pathology, Albert Einstein College of Medicine, Yeshiva University, New York

## ABSTRACT

In dorsal root ganglia and peripheral nerve of the rat and other species, nucleoside phosphatase and unspecific cholinesterase reaction products are found in the plasma membranes and spaces between them at two sites: (1) Schwann cell-axon interfaces and mesaxons of unmyelinated fibers, and (2) sheath cell-perikaryon interfaces and interfaces between adjacent sheath cells. Acetylcholinesterase reaction product is found in the perikaryon (within the endoplasmic reticulum) and the axon (axoplasmic surface). Nucleoside phosphatase reaction product is also found in the numerous vacuoles at the surface of perineurium cells, ganglion sheath cells, and cells surrounding some ganglion blood vessels. Nucleoside phosphatase activities in the sections fail to respond, in the manner described for "transport ATPase," to diisopropylphosphofluoridate, sodium and potassium ions, and ouabain. Nucleoside diphosphates are hydrolyzed more slowly than triphosphates in unmyelinated fibers, and are not hydrolyzed at the perikaryon surface. Nucleoside monophosphates are either not hydrolyzed or hydrolyzed very slowly. In contrast to these localizations, which are believed to demonstrate sites of enzyme activity, it is considered likely that diffusion artifacts account for the nucleoside phosphatase reaction product frequently found along the outer surfaces of myelinated fibers and within vacuoles at the Schwann cell surfaces of these fibers. The diffuse reaction product seen in basement membranes of ganglion and nerve may also be artifact.

Electron microscope examination of reaction product resulting from enzyme activities is becoming increasingly useful. Among the enzyme activities that can be studied are two which show significant localizations in nerve tissue: nucleoside phosphatase and cholinesterase.

We are reporting the direct demonstration of acetylcholinesterase at the axoplasmic surface of myelinated fibers. The studies described here also confirm and extend earlier observations that acetylcholinesterase activity is present in the endoplasmic reticulum of perikarya.

One of the most interesting aspects of the localizations being reported is the presence of unspecific cholinesterase activity and nucleoside phosphatase activity in identical sites in dorsal root ganglia and peripheral nerve, studied by both light microscopy and electron microscopy.

This communication emphasizes the usefulness of nucleoside phosphatase preparations for light microscope studies of nerve tissues, and it indicates the need for critical evaluation of observed sites of reaction product, particularly in electron

micrographs, for distinguishing diffusion artifacts from valid enzyme localizations.

## MATERIALS AND METHODS

Sprague-Dawley rats, of either sex, were used in all experiments. Also studied were several mice (CF1, C57 black, and A Jax); two rabbits (white albino); two cats; two frogs (*Rana pipiens*); and one toad (*Bufo marinus*).

Fixation of rat tissues was by perfusion, which preserved structure more satisfactorily than immersion fixation. For light microscopy, both 4% formaldehyde-1% calcium chloride (1) (4°C, 10 min perfusion, followed by overnight immersion) and 3% glutaraldehyde-0.1 M cacodylate buffer (38) (4°C, 10 min perfusion, followed by 20 min immersion) were used. For electron microscopy, glutaraldehyde perfusion was used, except where its inhibition of enzyme activity was excessive, as indicated in the next section.

The effect of fixation upon the localization and intensity of staining for nucleoside phosphatase and cholinesterase was also tested with 10- $\mu$  frozen sections cut from unfixed tissue in the Lab-Tek (Ames Co., Inc., Elkhart, Indiana) cryostat. These were incubated unfixed and following 15 min fixation in cold formaldehyde-calcium.

Nucleoside phosphatase activity was tested by incubation in the medium of Wachstein and Meisel (45), using manganese instead of magnesium ions as activator, with the following substrates: the triphosphates, diphosphates, and monophosphates of adenosine, guanosine, uridine, cytidine, and inosine; and thiamine pyrophosphate (26). The effects of diisopropylphosphofluoridate (DIPF) ( $1 \times 10^{-4}$  M), sodium ( $1 \times 10^{-1}$  M) and potassium ions ( $3 \times 10^{-2}$  M), and ouabain ( $2 \times 10^{-4}$  M) were tested in the adenosine triphosphate (ATP) medium, and also in two ATP media reported to permit demonstration of ion and ouabain sensitivity of enzyme activity (5, 18).

Unspecific cholinesterase and acetylcholinesterase activities were shown by the method of Karnovsky and Roots (16) and Karnovsky (15), using butyrylthiocholine iodide and acetylthiocholine iodide as substrates, respectively. The effects of two inhibitors upon their activities were also studied (by light microscopy only):  $1 \times 10^{-6}$  M to  $5 \times 10^{-5}$  M R020683 (Hoffman-LaRoche, Nutley, New Jersey), an inhibitor of unspecific cholinesterase, and  $2 \times 10^{-6}$  M to  $5 \times 10^{-4}$  M BW62C47 (Burroughs-Wellcome, Tuckahoe, New York), an inhibitor of acetylcholinesterase.

For demonstrating sites of enzyme reaction products at the electron microscope level, 40- $\mu$  frozen sections of glutaraldehyde-perfused tissues were prepared on the Sartorius microtome. Localizations of cholinesterase activities in spinal ganglia were also studied in sections (probably 50 to 100  $\mu$  thick) of

unfrozen glutaraldehyde-fixed tissue prepared with the Smith and Farquhar "chopper" (40). Following incubation for appropriate periods (monitored by light microscopy) in media to which 5% sucrose was added, tissues were rinsed in 7.5% sucrose, postfixed in osmium tetroxide buffered with veronal-acetate and containing sucrose (4), dehydrated in alcohols, and embedded in Araldite (10). Thin sections were cut in the Porter-Blum microtome, and examined unstained or stained by uranyl acetate (46) followed by lead citrate (35) for phosphatases, and unstained or stained with uranyl acetate for cholinesterases, in the RCA EMU-3B or Siemens Elmiskop I.

## RESULTS

### *Effects of Fixation*

The *distributions* of reaction products, at the light microscope level, are the same whether cryostat sections are incubated unfixed or following formaldehyde-calcium fixation. No structure is stained in unfixed tissue that is not also stained in the fixed tissue. The *level* of activity, as judged by intensity of "staining," is essentially the same in fixed and unfixed sections in the case of unspecific cholinesterase and acetylcholinesterase activities, and is higher in fixed tissue in the case of nucleoside phosphatase activities. The increased intensity can probably be attributed to better survival of cell structure during incubation and a reduction in enzyme loss to the medium. A dramatic instance of the influence of structural integrity upon staining intensity is seen with neurons of frog dorsal root ganglia, fixed by immersion. The cytoplasmic staining for acetylcholinesterase activity is much more intense following glutaraldehyde than formaldehyde fixation (Figs. 23 and 24). This may also be the reason why the staining for nucleoside phosphatase activity in rat unmyelinated fibers is somewhat darker following glutaraldehyde than formaldehyde fixation (perfusion). A similar finding at the electron microscope level is the marked improvement in localization of cholinesterase reaction product when chopper sections of ganglia are used rather than frozen sections. Structural preservation is considerably better in the chopper sections of ganglia.

Increased "staining" intensity resulting from fixation has previously been reported for a variety of enzymes: oxidative enzymes (27, 29), nucleoside diphosphatase and thiamine pyrophosphatase (28), esterases (12, 7), glucose-6-phosphatase (12), and sulfatase (11).

Glutaraldehyde fixation virtually abolishes nucleoside phosphatase activity in the perineurium cells and ganglion sheath cells in mammals (negative after 45 min incubation at 37°C). As previously reported for blood capillaries of other tissues (12), glutaraldehyde strongly inhibits nucleoside phosphatase activity in capillaries of ganglia and sciatic nerve.

#### *Nucleoside Phosphatase Activity in the Rat*

**LIGHT MICROSCOPY.** Following formaldehyde or glutaraldehyde fixation, unmyelinated fibers in dorsal root ganglia and sciatic nerve stain rapidly when incubated with any of the nucleoside triphosphates tested, even near 0°C (Figs. 1, 7). Prolonged incubation at 37°C (Fig. 2), even to the point at which the preparation is no longer useful for the unmyelinated fibers, fails to stain the myelinated fibers (*see* reference 24, Figs. 9 and 10).

A narrow region surrounding the perikarya of the neurons in the ganglia also stains intensely with nucleoside triphosphates (Figs. 1 and 2). Not all neurons are equally active in this regard.

When a nucleoside diphosphate or thiamine pyrophosphate is substituted for a triphosphate, unmyelinated fibers show activity but this activity is considerably less than with triphosphates (Figs. 4, 8).<sup>1</sup> No staining occurs at the perikaryon surface with diphosphates (Figs. 3, 4), even after 30 min at 37°C. As with triphosphates, myelinated fibers are unstained even after long incubation at 37°C.

With nucleoside monophosphates as substrate, these sites are negative after 15 to 45 min of incubation at 37°C (Fig. 5). Slight activity is present in isolated regions of some of the larger blood vessels and what appears to be fibrous tissue of sciatic nerve; electron microscopy is required to establish the identity of these stained cells. Prolonging the incubation to an hour or more results in the light staining of ganglion capsule and perineurium (Fig. 9), and very light staining of unmyelinated fibers. Lysosomes and related structures of neurons are also stained with longer incubations, especially in sections of formaldehyde-fixed tissue (*see* reference 24, Fig. 13).

Blood capillaries, perineurium, and ganglion

<sup>1</sup> A publication by Rostgaard and Barnett (37) which appeared while this paper was in preparation reports nucleoside triphosphatase and diphosphatase activities in unmyelinated nerve fibers of rat intestine.

capsule hydrolyze nucleoside triphosphates rapidly, and diphosphates to a lesser degree.

Compared to formaldehyde, glutaraldehyde yields slightly more intensely stained unmyelinated fibers. Because glutaraldehyde at the same time abolishes perineurium and capsule staining and markedly decreases blood vessel staining, the contrast between unmyelinated fibers and other structures is greater in glutaraldehyde-fixed ganglia and nerve than in formaldehyde-fixed tissue.

Pretreatment in  $1 \times 10^{-4}$  M DIFP for 30 min at room temperature (32) has no inhibitory effect on the nucleoside triphosphatase activities in ganglion and sciatic nerve. This is true whether the tissue is unfixed or fixed prior to treatment and incubation (Fig. 1).

Tests with nucleoside phosphatase activity in sections of unfixed and fixed ganglia and sciatic nerve (also kidney and several other tissues) fail to reveal the stimulation by sodium and potassium ions and inhibition by ouabain characteristic of "transport ATPase." This is true not only in the Wachstein-Meisel method, as previously reported for several tissues (30), but also in the two variants of this procedure recently proposed to demonstrate these responses to ions and cardiac glycoside (5, 18). In our hands, the glycoside leads to a slightly more *intense* staining with the two recently proposed systems; and sodium and potassium ions produce a similar effect in one of the systems (18). However, we consider it probable that the slight differences are due to effects upon the precipitation that occurs when the media are prepared, which is massive with one of them (5). Alteration of either lead or substrate concentration could affect reaction product (lead phosphate) precipitation in the sections during incubation.

**ELECTRON MICROSCOPY:** None of the sites that is negative by light microscopy reveals reaction product when viewed by electron microscopy. Thus, with adenosine triphosphate as substrate, much reaction product is found at the perikaryon-sheath cell interface (Fig. 10), but there is none with adenosine diphosphate (Fig. 11; *see* also reference 24, Fig. 25).

Incubations at ice temperature are useful for finding the first sites of reaction product deposition. In unmyelinated fibers, the initial sites are the membranes, and spaces between them, at Schwann cell-axon interfaces and mesaxons (Fig. 12). Surrounding the perikarya, they are the mem-

branes, and spaces between them, at the sheath cell-neuron interfaces and the interfaces between adjacent sheath cells (Fig. 12; see also reference 24, Fig. 22). Occasionally, reaction product is observed on small regions of the membranes and not in the interspaces between them.

Diffuse reaction product is seen in the basement membranes surrounding unmyelinated fibers and sheath cells (Figs. 10, 11, 14, and 15). However, firmer evidence seems desirable before it is concluded that basement membranes possess nucleoside phosphatase activity, because: (1) the amount of product decreases in gradient fashion as the distance from the initial sites increases (Fig. 14); and (2) the product is either absent or virtually so when the initial sites show slight activity (Fig. 12) and it becomes more marked with increasing incubation time.

A more clearly artifactual deposit of reaction product is encountered along myelinated fibers, at the outer surfaces of the Schwann cells and in small pinocytoticlike vacuoles along these surfaces

(Figs. 14 to 17). The following observations make it likely that these deposits result from diffusion of lead phosphate from sites of high activity to the Schwann cell surfaces and associated vacuoles: (1) These deposits are never seen as initial sites; whenever the deposits are seen there are always unmyelinated fibers or sheath cells nearby, with much heavier accumulations of product. (2) The incidence of deposits along myelinated fibers becomes higher as initial sites show heavier accumulations. (3) When one aspect of a myelinated fiber faces an initial site with reaction product and another aspect faces away from such a site, the remote aspect shows no reaction product while the adjacent aspect shows it. (4) Reaction product is found at the outermost surface of the myelinated fiber, and almost never within the myelin. (5) Prolonged incubations, up to twenty times those yielding the reaction product seen against myelinated fibers in the electron microscope, fail to produce reaction product inside

---

FIGURE 1 Dorsal root ganglion, rat. Fixation: formaldehyde-calcium perfusion. Incubation: ATP medium, 0°C, 10 min. Reaction product between neuron perikarya (*P*) and sheath cells seen at arrows and elsewhere; "stained" blood capillaries are seen at *C* and elsewhere.  $\times 470$ .

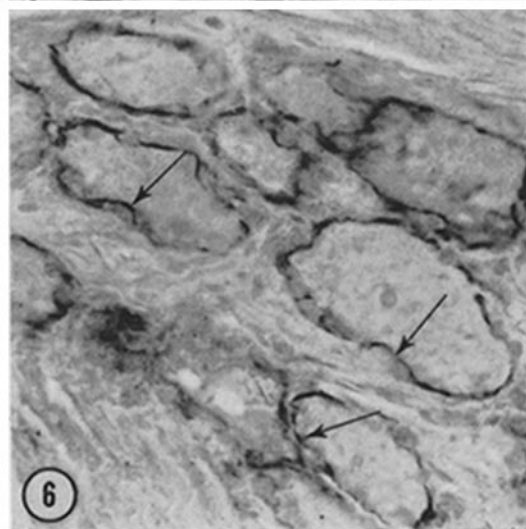
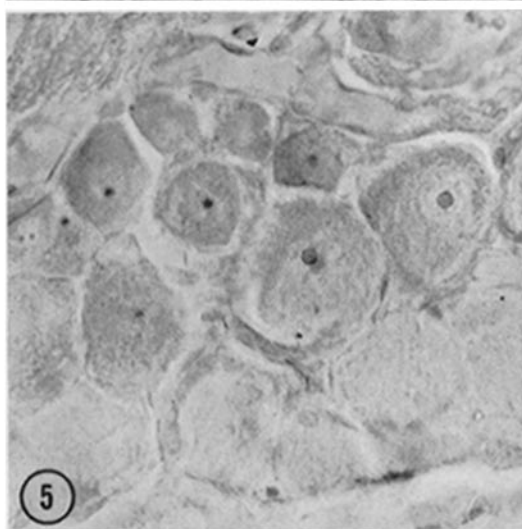
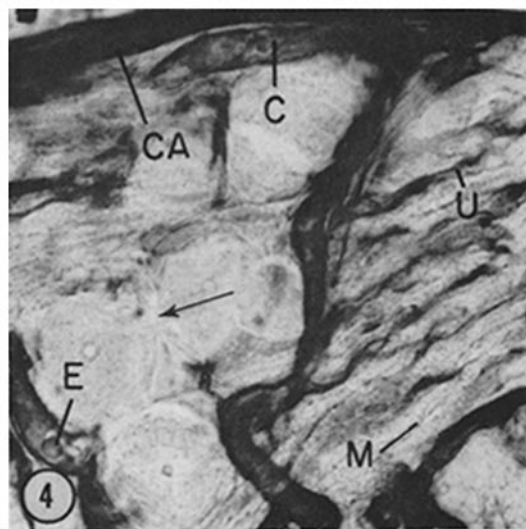
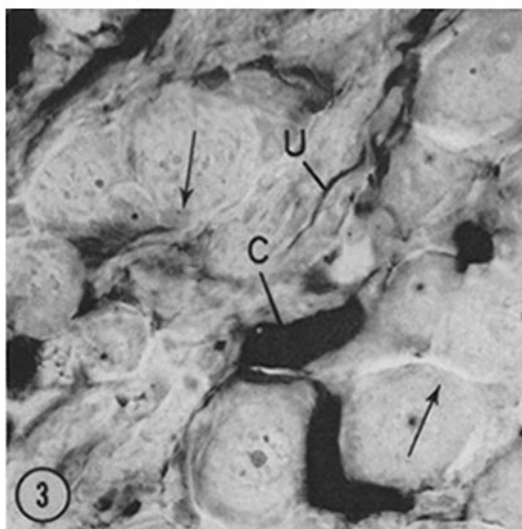
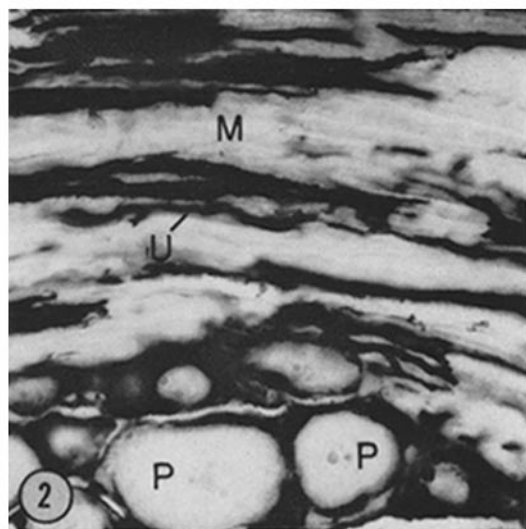
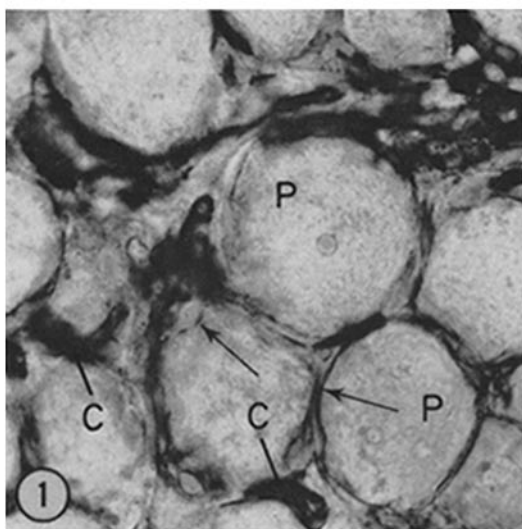
FIGURE 2 Dorsal root ganglion, rat. Fixation: glutaraldehyde-cacodylate perfusion. Incubation: ATP medium, 37°C, 15 min. Intense accumulations of reaction product are present around perikarya (*P*) and in unmyelinated nerve fibers (*U*) but none is seen in myelinated fibers (*M*).  $\times 370$ .

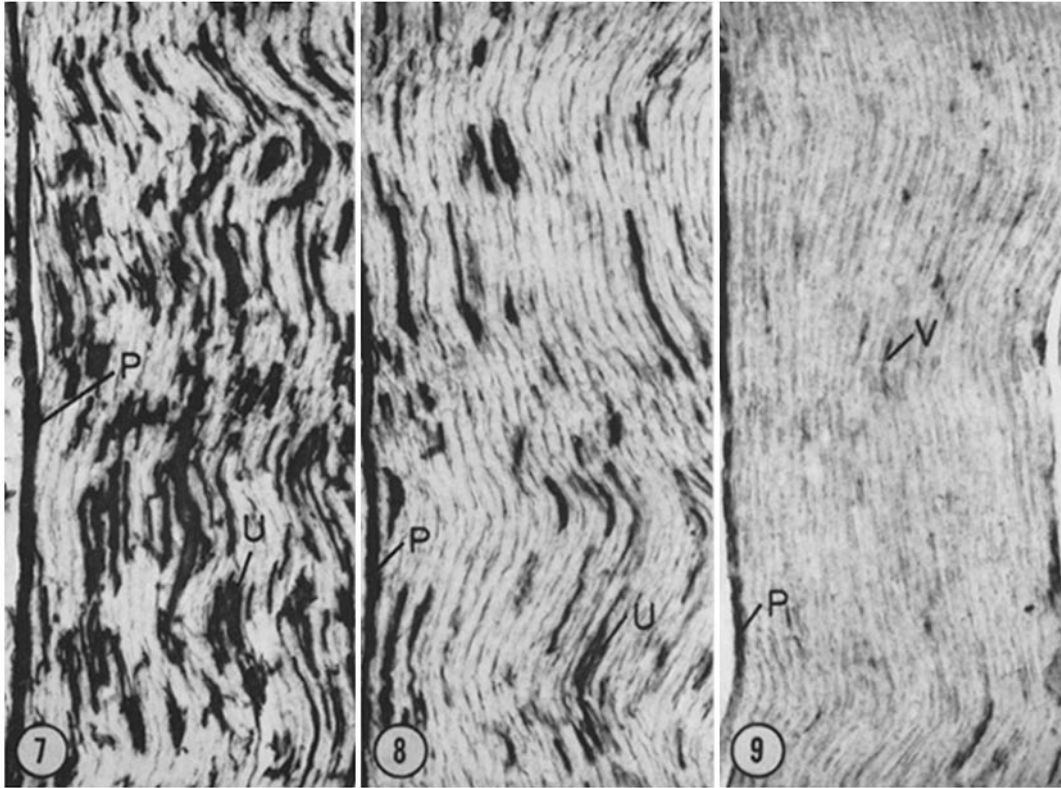
FIGURE 3 Dorsal root ganglion, rat. Fixation: formaldehyde-calcium perfusion. Incubation: adenosine diphosphate medium, 37°C, 15 min. Blood capillaries (*C*) are intensely stained; unmyelinated fibers (*U*) are stained; but no stain is present surrounding the perikarya (arrows and elsewhere).  $\times 500$ .

FIGURE 4 Dorsal root ganglion, rat. Fixation: formaldehyde-calcium perfusion. Incubation: adenosine diphosphate medium, 37°C, 10 min. Note staining of capsule (*CA*), blood vessels (*C*) and unmyelinated fibers (*U*). Myelinated fibers (*M*) are unstained. The erythrocyte (*E*) shows reaction product at its surface, but this may be a diffusion artifact (reference 21; cf. reference 42).  $\times 390$ .

FIGURE 5 Dorsal root ganglion, rat. Fixation: glutaraldehyde-cacodylate perfusion. Incubation: adenosine monophosphate medium, 37°C, 15 min. All structures that are stained with ATP (Figs. 1, 2) or adenosine diphosphate (Figs. 3, 4) are now unstained; prolonging the incubation time to 60 min. results in slight staining of capsule (see Fig. 9) and unmyelinated fibers.  $\times 400$ .

FIGURE 6 Dorsal root ganglion, cat. Fixation: glutaraldehyde-cacodylate immersion. Incubation: adenosine monophosphate, 37°C, 30 min. Reaction product is seen at the perikaryon surfaces.  $\times 400$ .





FIGURES 7 to 9 Sciatic nerve, rat. Fixation: formaldehyde-calcium perfusion. Incubation: Fig. 7, adenosine triphosphate, 25°C, 15 min.; Fig. 8, adenosine diphosphate, 25°C, 15 min.; Fig. 9, adenosine monophosphate, 37°C, 60 min. The perineurium (*P*) is stained intensely with the triphosphate and diphosphate and lightly with the monophosphate. Unmyelinated fibers (*U*) stain intensely with the triphosphate, considerably less with the diphosphate, and very lightly with the monophosphate. A blood vessel is seen at *V*. Myelinated fibers are unstained with all three substrates.  $\times 170$ .

these fibers when viewed in the light microscope (Fig. 2).

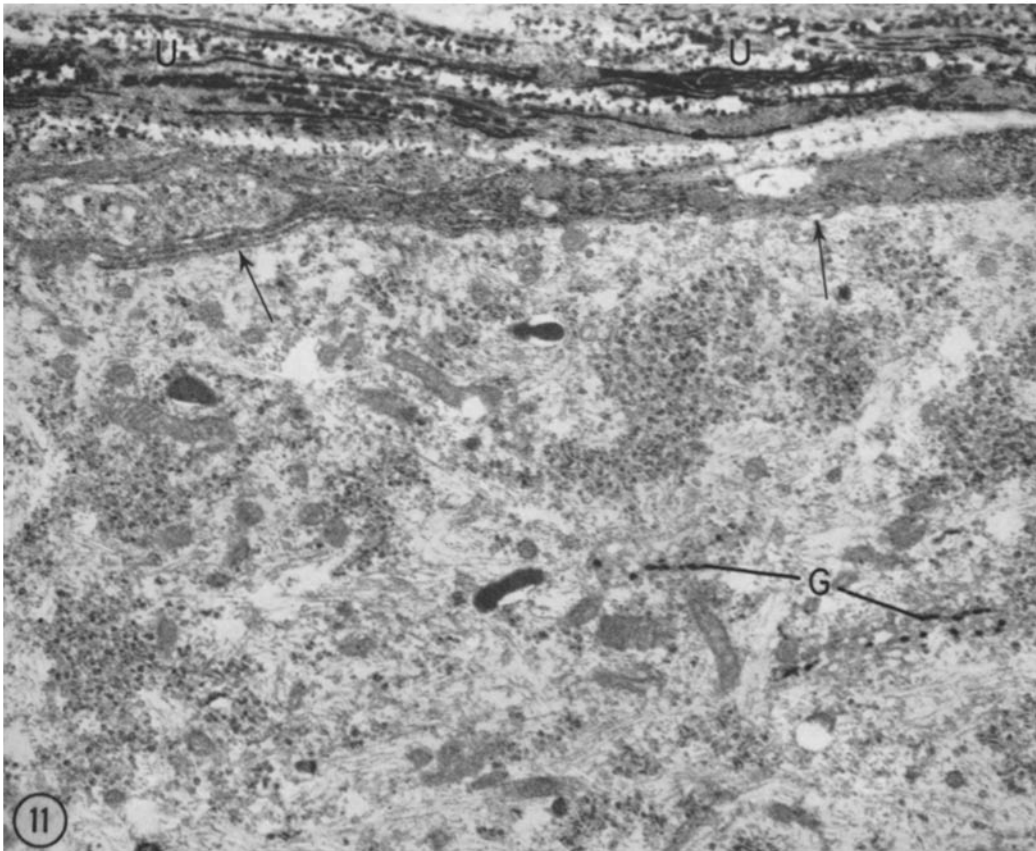
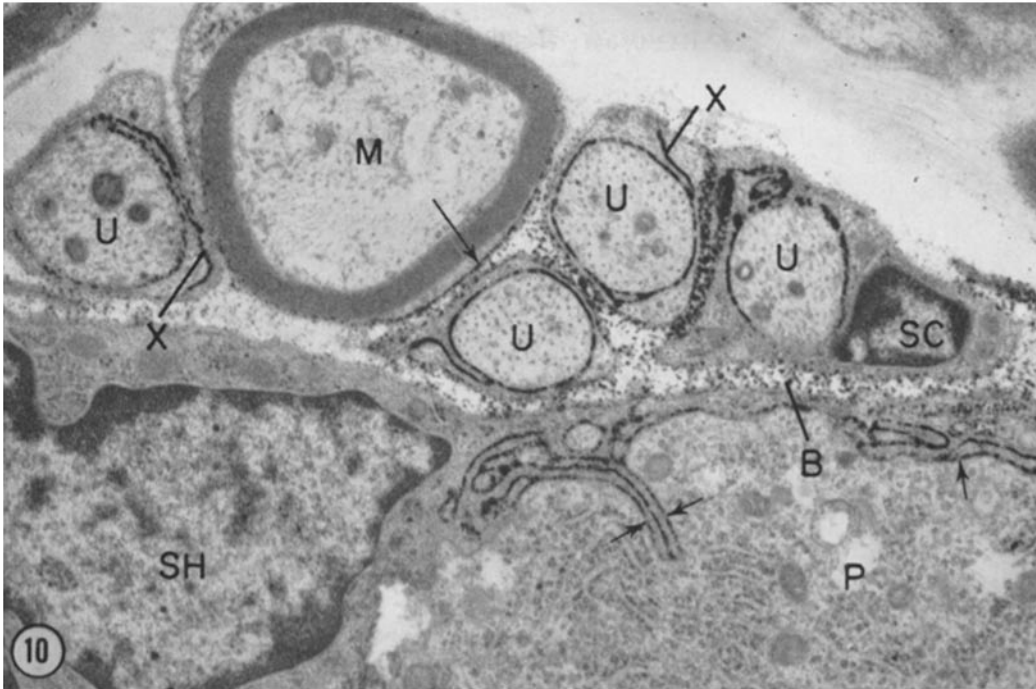
It is the *inner* surfaces which are the sites of activity in Schwann cells of unmyelinated fibers

and in sheath cells. The presence of reaction product on the *outer* surface of myelinated fibers, and only when these lie adjacent to unmyelinated fibers with high activity, argues strongly against

---

FIGURE 10 Dorsal root ganglion, rat. Incubation: ATP medium, 37°C, 8 min. Reaction product is seen: (1) at short arrows, between perikaryon (*P*) and sheath cell (its nucleus is labeled *SH*); (2) between axoplasm of unmyelinated fibers (*U*) and Schwann cell (its nucleus is labeled *SC*); (3) at mesaxons of unmyelinated fibers (*X*); (4) at basement membrane (*B*); and (5) at the outer surface (long arrow) of myelinated fiber (*M*). See text for discussion of localizations (4) and (5).  $\times 13,500$ .

FIGURE 11 Dorsal root ganglion, rat. Incubation: adenosine diphosphate medium, 25°C, 45 min. Much reaction product is seen in unmyelinated fibers (*U*) but none is present at the perikaryon-sheath cell interfaces (arrows). Some reaction product is present in Golgi saccules (*G*).  $\times 11,000$ .



an alternative conclusion, namely that an enzyme is, in fact, localized in the myelinated fiber, but the demonstration of its reaction product requires peculiarly high concentration of lead phosphate that arises only near initial sites with high levels of enzyme activity.

Electron microscopy of the perineurium and ganglion capsule shows the nucleoside phosphatase reaction product to be restricted to the micro-pinocytoticlike vesicles found at the cell surfaces in large numbers (*see* reference 24, Figs. 27, 28).

Specific mention should be made of some sites that show no reaction product for nucleoside phosphatase. Two of these are areas in myelinated fibers in which the myelin is differently arranged (Schmidt-Lanterman incisures) or absent (nodes of Ranvier). Were high phosphatase activity localized there, it might suggest that different transport or other mechanisms are present where access to the axoplasmic surface from the exterior is greater. Although light microscopy reveals no reaction product at these sites, even after relatively long incubations, areas below the resolving power of the instrument would go unnoticed. Therefore, both clefts and nodes were examined by electron microscopy. In no case is reaction product found at the axonal surface, either at the incisures or nodes (Figs. 18, 19). Sometimes, slight deposits are encountered at the periphery of the Schwann cell (Figs. 18, 19), but these, for reasons considered when describing myelinated fibers generally, are considered to be diffusion artifacts.

Other sites without reaction product are two regions of endoplasmic reticulum, the subsurface cisternae in the perikaryon (36), and the reticulum within the axons (Fig. 14). Nowhere in the neuron does the endoplasmic reticulum give evidence of nucleoside phosphatase activity.

No differences are discernible between the nucleoside phosphatase activities in the regions of plasma membrane lying above the subsurface cisternae and that in the membrane generally.

#### *Cholinesterase Activities in the Rat*

**LIGHT MICROSCOPY:** Unspecific cholinesterase is distinguished from the acetylcholinesterase in the present experiments by the following criteria: (1) the unspecific enzyme readily hydrolyzes butyrylthiocholine iodide (Fig. 22); (2) its activity is unaffected by  $5 \times 10^{-4}$  M 62C47, whereas acetylcholinesterase activity is totally inhibited at  $2 \times 10^{-5}$  M (Fig. 21); and (3) it is inhibited by RO 20683, an inhibitor of unspecific cholinesterase activity, markedly at  $1 \times 10^{-6}$  M and completely at  $1 \times 10^{-5}$  M.

In contrast to nucleoside phosphatase activity, unspecific cholinesterase activity (also acetylcholinesterase activity) is irreversibly inhibited by pretreating frozen sections, of fixed or unfixed tissues, with  $1 \times 10^{-4}$  M DIPP for 30 min at room temperature, as in the studies of Ostrowski and Barnard (32, 33) with esterases of motor endplates and kidney.

Unspecific cholinesterase activity shows the same localizations as seen for nucleoside phosphatase activity. Thus, irrespective of whether butyrylthiocholine iodide, acetylthiocholine iodide or methoxy acetyl- $\beta$ -methyl thiocholine iodide is used as substrate, or whether the inhibitor BW 62C47 ( $5 \times 10^{-4}$  M) is present or not, a brown deposit forms in unmyelinated fibers and in sheath cells surrounding the perikarya (Figs. 20 to 22, 25, and 26).

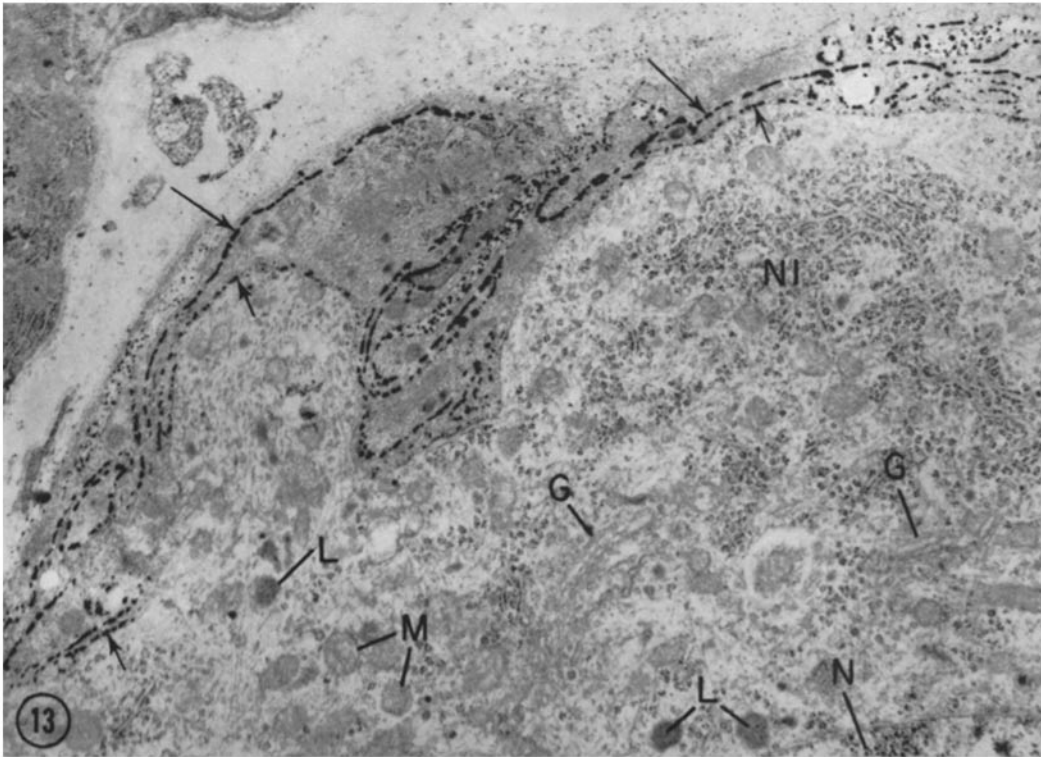
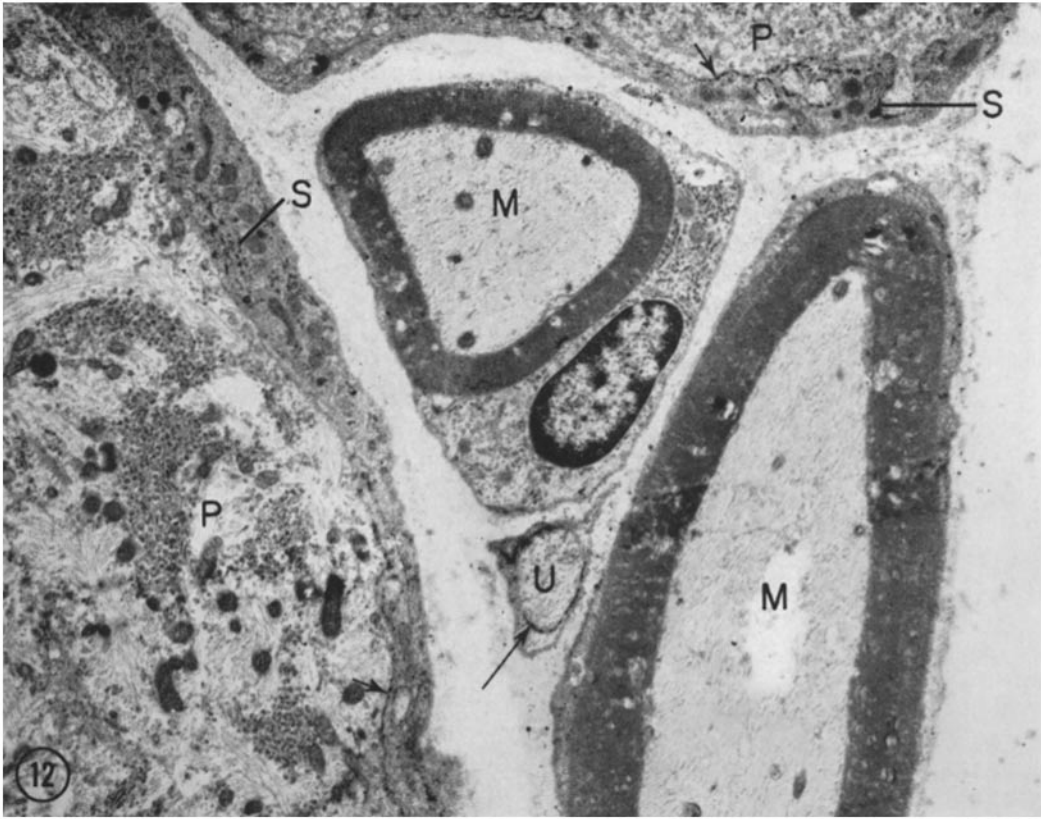
Acetylcholinesterase activity is revealed in the perikaryon cytoplasm (Fig. 20) and at the axoplasmic surfaces of myelinated fibers (Figs. 25,

---

FIGURE 12 Dorsal root ganglion, rat. Incubation: ATP medium, 3°C, 5 min. Reaction product is seen: (1) surrounding perikarya (*P*), between the cell surface and enclosing sheath cells (short arrows); (2) between adjacent sheath cells (*S*); and (3) between Schwann cell and axoplasm of unmyelinated nerve fiber (*U*), at long arrow. Note absence of reaction product from myelinated fibers (*M*).  $\times 6,200$ .

FIGURE 13 Dorsal root ganglion, rat. Incubation: ATP medium, 37°C, 8 min. The origin of the neurite from the perikaryon of the neuron is seen. In the perikaryon, the following structures are without reaction product: *G*, Golgi apparatus; *L*, lysosomes; *M*, mitochondria; *N*, nucleus; *NI*, Nissl material. Reaction product is present in the spaces between perikaryon and neurite and surrounding sheath cells (short arrows) and between adjacent sheath cells (long arrows).  $\times 10,000$ .





26). Staining occurs when either acetylthiocholine iodide or methoxy acetyl- $\beta$ -methyl thiocholine iodide is used as substrate but not when butyrylthiocholine iodide is substituted for them (Fig. 22). It is unaffected by  $1 \times 10^{-6}$  M RO 20683 and only moderately inhibited at  $1 \times 10^{-5}$  M and  $5 \times 10^{-5}$  M. It is totally inhibited by  $2 \times 10^{-5}$  M BW 62C47 (Fig. 21).

Cholinesterase activity is seen in all perikarya, but at greatly differing levels (Figs. 20, 23). Not all myelinated fibers show acetylcholinesterase activity at the axoplasmic surface by light microscopy; this is particularly true of the sciatic nerve in which structural preservation is less adequate than in the nerves within the spinal ganglia. However, when the sciatic nerve is crushed (22), the myelinated fibers proximal to the crush show increased staining for acetylcholinesterase activity and now all axoplasmic surfaces show activity.

The activity in unmyelinated fibers with acetylthiocholine iodide as substrate appears due, largely or exclusively, to the unspecific cholinesterase since it is markedly or completely inhibited by  $1 \times 10^{-6}$  M RO 20683, whereas the acetylcholinesterase of perikarya requires 10 to 50 times the concentration for only moderate inhibition.

**ELECTRON MICROSCOPY:** By incubating at ice temperature, diffusion of reaction product is reduced but not eliminated (Fig. 27). As indicated earlier, localizations are sharper with chopper sections than with frozen sections.

The localizations of reaction product from *unspecific* cholinesterase activity corresponds to those from nucleoside phosphatase activities: the plasma membranes and spaces between them at two sites, the Schwann cell-axon interfaces and interfaces of adjacent sheath cells (Figs. 27 to 30).

The localization of cholinesterase activity is

striking under the electron microscope: at the axoplasmic surface of myelinated fibers (Figs. 29, 30), and in the endoplasmic reticulum membranes and spaces between them (Fig. 28). The nuclear envelope behaves like the rest of the endoplasmic reticulum in this respect (Fig. 28).

#### *Localizations in Other Species*

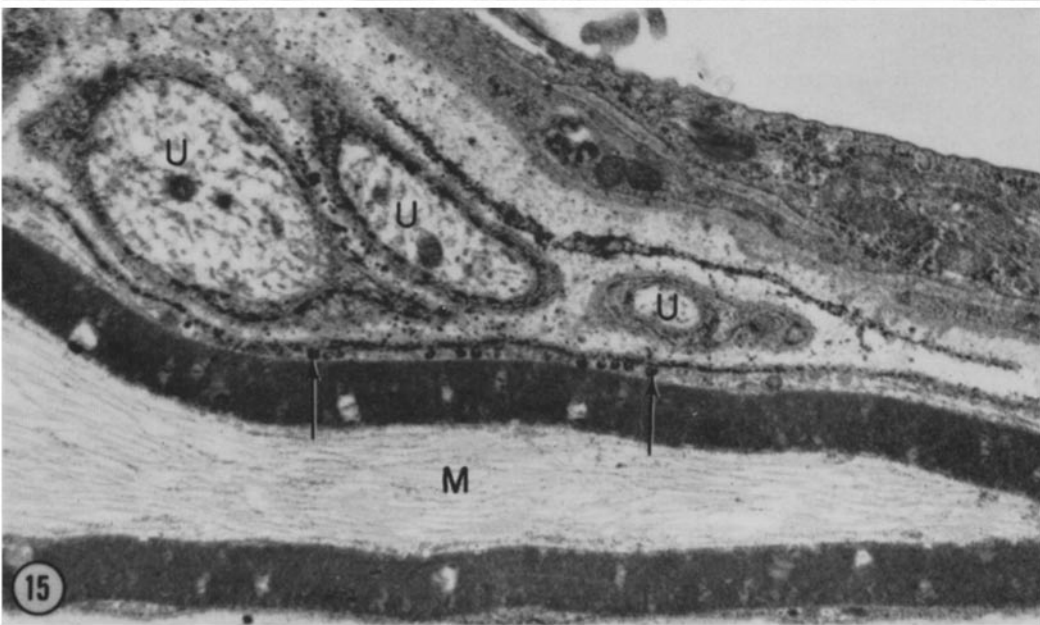
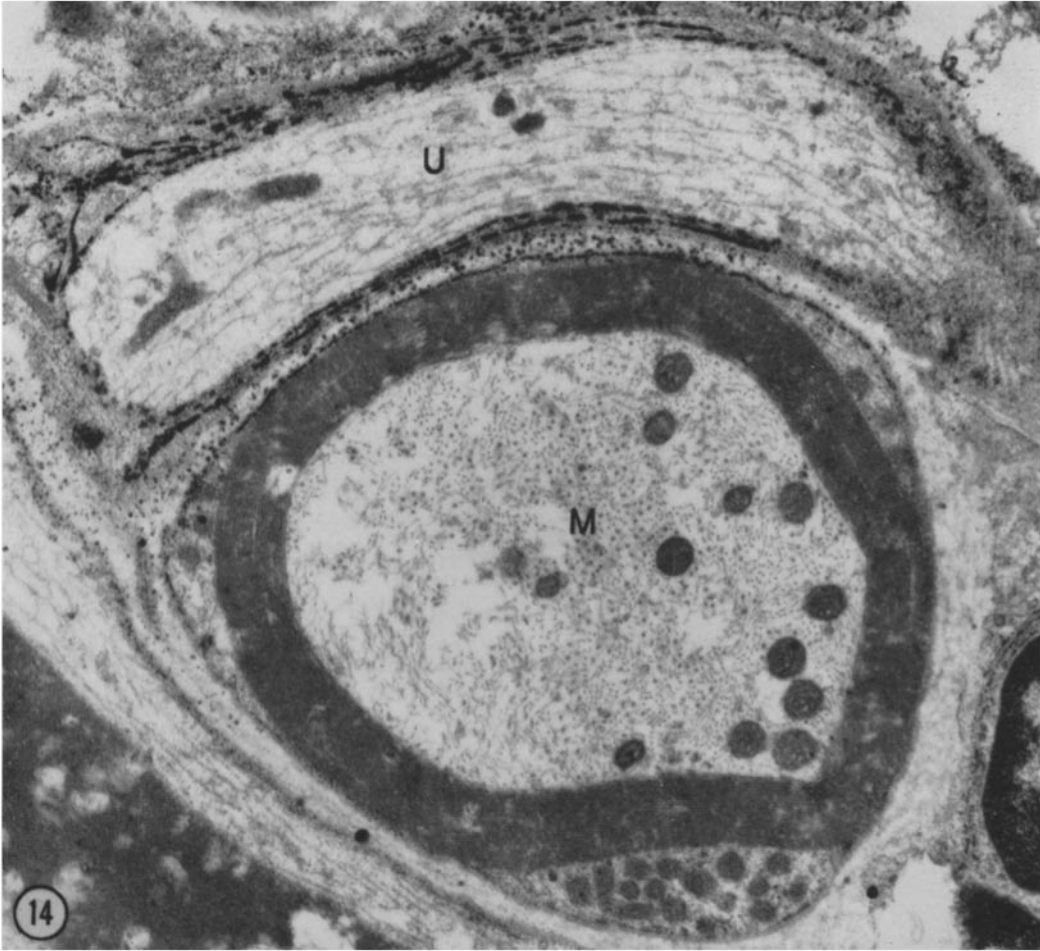
The relatively limited observations made on three other mammals and two amphibia (with the mono-, di-, and triphosphates of adenosine and inosine) are similar to those described for the rat. In all instances, myelinated fibers show no activity. Unmyelinated fibers and perikaryon-sheath cell surfaces are strongly stained with triphosphates and diphosphates, except in the cat and frog in which the diphosphates appear not to be split. Furthermore, the reaction product with triphosphates is so limited that electron microscopy would be highly desirable to establish that it is, in fact, localized in unmyelinated fibers and not, for example, in connective tissue cells. In the cat, there is strong nucleoside monophosphatase activity at the perikaryon-sheath cell surfaces (Fig. 6); to a lesser degree, this is true also in the rabbit.

Unspecific cholinesterase activity (butyrylthiocholine iodide and acetylthiocholine iodide as substrates; specific inhibitors not tested) is localized at the perikaryon-sheath cell interfaces and in unmyelinated fibers (Fig. 26), while acetylcholinesterase (acetylthiocholine iodide as substrate; inhibitors untested) is present at the axoplasmic surfaces of myelinated fibers (Fig. 26) and in the perikaryon cytoplasm (Fig. 23). The staining intensity resulting from acetylcholinesterase at the axoplasmic surface is much stronger in the mouse (Fig. 26), rabbit, and frog than in the rat. In the

---

**FIGURE 14** Dorsal root ganglion, rat. Incubation: ATP medium, 3°C, 5 min. Reaction product is absent from the myelinated fiber (*M*) except where it is adjacent to the unmyelinated fiber (*U*) with its reaction product. Reaction product is also present in the basement membrane adjacent to the unmyelinated fiber. The diagonal lines seen in the myelin sheath are artifacts of the engraving process.  $\times 13,500$ .

**FIGURE 15** Dorsal root ganglion, rat. Incubation: ATP medium, 3°C, 5 min. The myelinated fiber (*M*) shows no reaction away from the unmyelinated fibers (*U*) with their reaction product. However, the surface facing the unmyelinated fiber shows reaction product, including the small vacuoles seen between the two arrows. Some reaction product is present in the basement membrane between unmyelinated and myelinated fibers, but not on the other side of the myelinated fiber.  $\times 9,900$ .



cat, unmyelinated fibers are positive when acetylthiocholine iodide is used as substrate but are negative with butyrylthiocholine iodide (up to 3 hr at 25°C).

An incidental observation is the staining of the lysosomes of perikarya in amphibian spinal ganglia when nucleoside triphosphates are used as substrates at neutral pH, circumstances under which mammalian perikaryon lysosomes show no activity. This is particularly interesting since the perikaryon lysosomes of amphibians resemble those of mammals in not hydrolyzing nucleoside diphosphates under these conditions.

#### DISCUSSION

The striking correspondence in the localizations of unspecific cholinesterase and nucleoside phosphatase activities raises the question as to whether both are properties of the same enzyme. Such identity seems unlikely, particularly because of the differential effect of pretreating sections with DIFP before incubation: the cholinesterase activity is completely and irreversibly inhibited while the nucleoside phosphatase activity is unaffected. However, until the enzyme activities are tested in isolated, purified preparations, it is best to qualify this conclusion since, as soon to be considered in another connection, the possibility exists that the incubation medium alters the properties of the phosphatase activity.

Whether one or more enzymes are involved, there may well be functional significance in the coincidence of cholinesterase and phosphatase localizations. Speculation regarding such significance is difficult since no information is available regarding the role of either activity in cell metabolism. Both cholinesterase and "transport ATPase" are considered to be localized in the membrane of

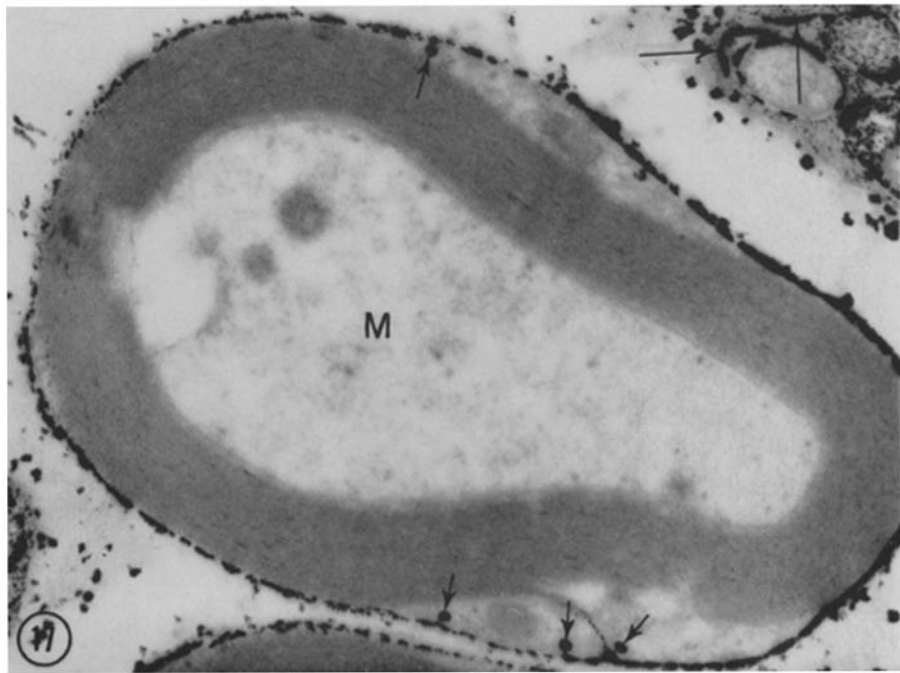
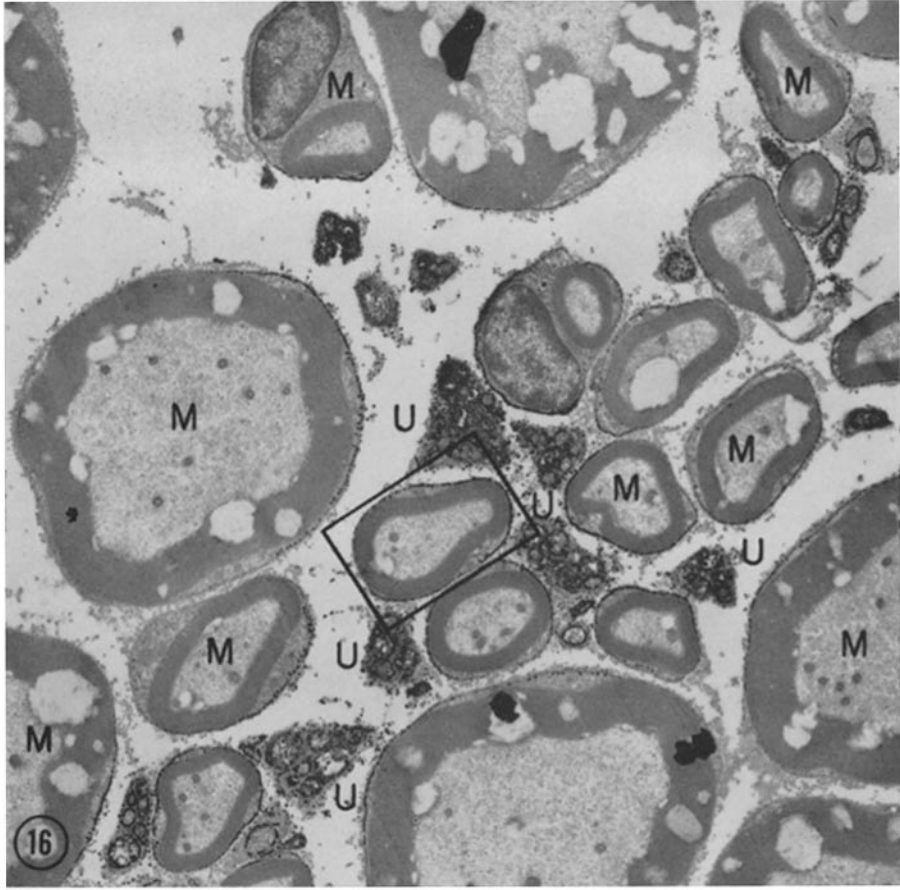
the red blood cell where they may influence cell permeability. It is not clear whether any of the nucleoside phosphatase activities demonstrable by in situ staining techniques is a "transport ATPase," identical with or similar to that studied by biochemists (39, 34, 6, 3). Unlike the biochemist's transport enzyme, the one(s) shown in situ rapidly hydrolyzes all nucleoside triphosphates and not infrequently, as in unmyelinated fibers, also diphosphates (2, 30, 31). Calcium ions, which inhibit the transport enzyme of biochemists, enhance staining in situ nearly as well as magnesium and manganese ions (30). In previous experiments, we have been unable to show significant effects of either sodium and potassium ions or ouabain (30, 31). Even drastic alterations of the incubation media recently reported to show such effects (5, 18) fail to do so in the current experiments. Possibly the lead ions of the incubation medium, or some other feature of the procedure, alter tissue or enzyme so that the enzyme acquires different properties. Yet it is equally possible that the enzyme(s) demonstrable in situ is not a transport enzyme as generally understood today.<sup>2</sup> If so, there is no clue to the functional

<sup>2</sup> While this manuscript was in preparation, Hokin and Yoda (13) reported that transport ATPase, in a membrane preparation prepared from kidney homogenates, is irreversibly inactivated by diisopropylphosphorofluoridate (DIPF) whereas nontransport ATPase activity, which can be separated from the membrane fraction by treatment with 0.6 M NaI, is unaffected by DIPF. The in situ enzyme(s) is unaffected by DIPF at concentrations that totally inhibit cholinesterase activity in the sections. The transport ATPase of Hokin and Yoda hydrolyzes GTP, CTP, and UTP at rates ranging from 6 to 0.3% of the rate of ATP hydrolysis; ADP is hydrolyzed at about 15% of the rate of ATP.

---

FIGURE 16 Nerve root of dorsal root ganglion, rat. Incubation: ATP medium, 25°C, 11 min. Spaces between fibers are artifacts probably arising in preparation of the frozen section. Note heavy accumulations of reaction product in unmyelinated fibers (*U*). In the myelinated fibers marked *M*, it is evident that reaction product has accumulated at the surfaces facing unmyelinated fibers but none is present at the surfaces facing away from unmyelinated fibers. Some reaction product is also present in the basement membrane between myelinated and unmyelinated fibers.  $\times 6,000$ .

FIGURE 17 Enlargement of rectangular area of Fig. 16. Reaction product is seen, in unmyelinated fibers, between plasma membranes of axons and Schwann cells (unlabeled) and in mesaxons (long arrows); and at the surfaces of myelinated fibers (*M*), including vacuoles (short arrows).  $\times 29,000$ .



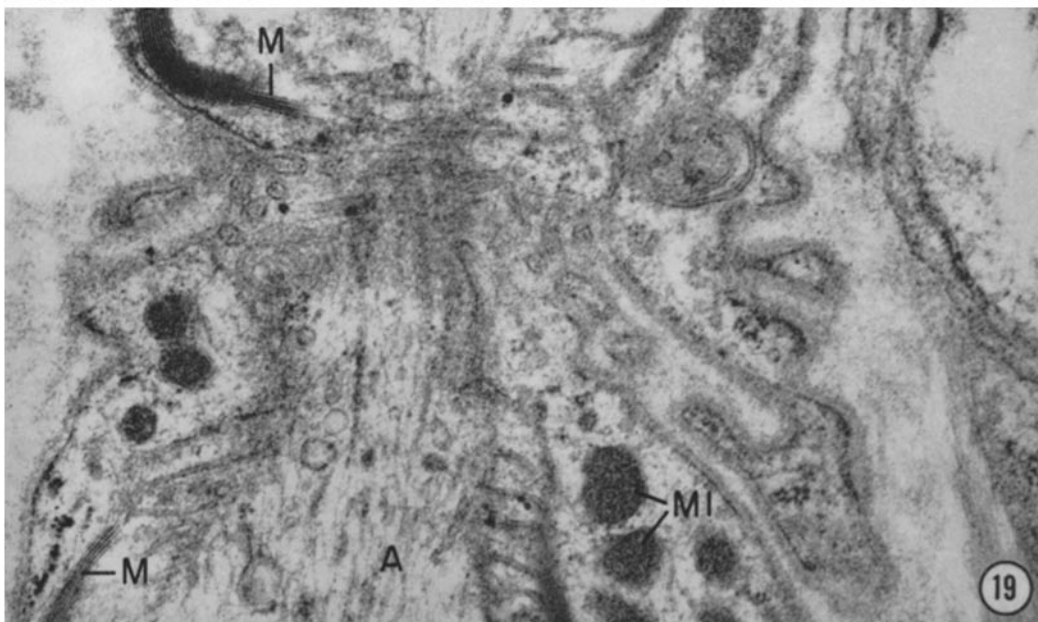
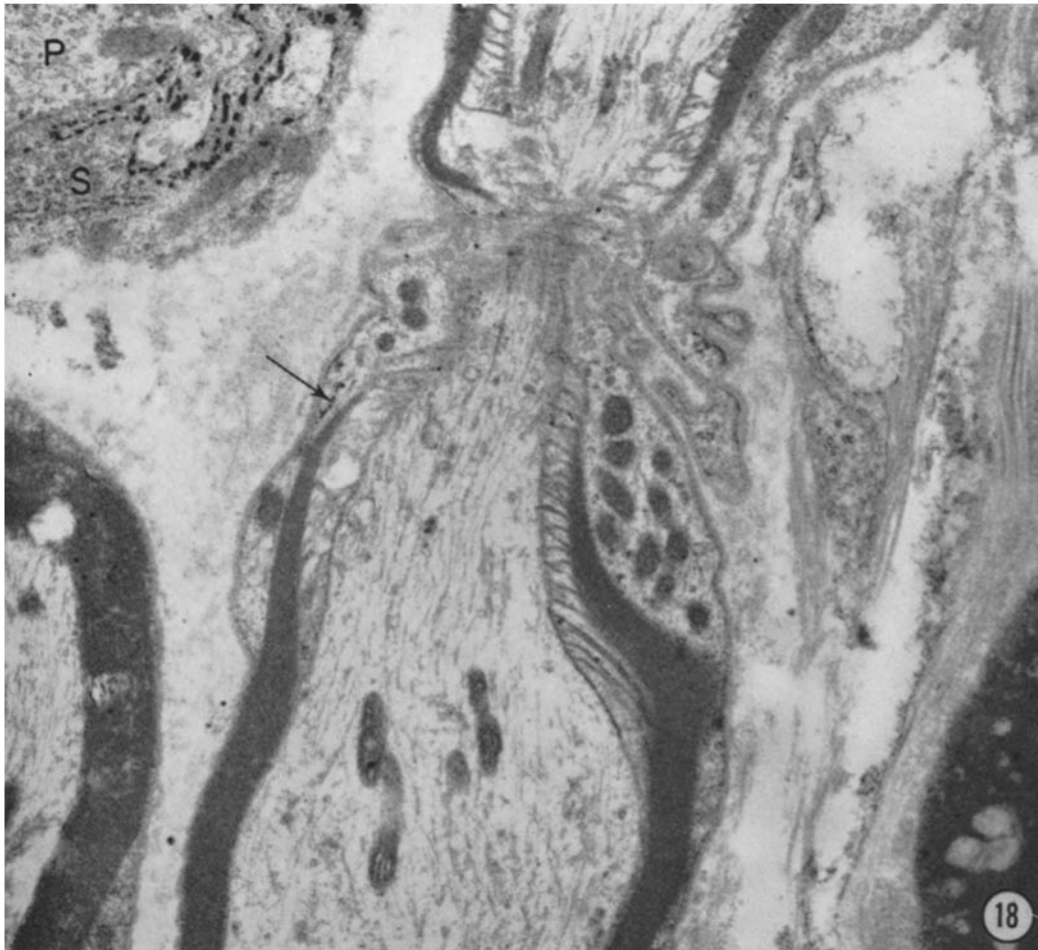


FIGURE 18 Dorsal root ganglion, rat. Incubation: ATP medium, 37°C, 8 min. Reaction product is present between plasma membranes of perikaryon (*P*) and sheath cell (*S*). The node of Ranvier lacks reaction product. The arrow indicates reaction product that, for reasons given in the text, is considered likely to be artifact rather than enzyme site.  $\times 14,000$ .

FIGURE 19 Enlargement of node area in Fig. 18. Reaction product is not seen in or near node of Ranvier. The following structures are labeled: *A*, axoplasm; *M*, myelin; and *MI*, mitochondria.  $\times 30,000$ .

significance of these phosphatases that are part of or close to the plasma membranes of neurons.

It is likely that triphosphatases rather than less specific nucleoside phosphatases are present at the perikaryon-sheath cell surfaces and in unmyelinated fibers of rabbit thoracic vagus, because triphosphates are hydrolyzed at these sites but not diphosphates. In contrast, in unmyelinated fibers of sciatic nerve and dorsal root ganglia and in perineurium cells, both diphosphates and triphosphates are hydrolyzed, and even monophosphates to a limited degree; at these sites one or more phosphatases may be present. Hydrolysis of monophosphates, but not diphosphates at the perikaryon-sheath cell surfaces in cat dorsal root ganglia suggests the presence of a monophosphatase. These and other indications of substrate specificities clearly require analysis in isolated enzyme preparations. Then it may be possible to evaluate the significance of species differences.

Another uncertainty regarding the phosphatases that we are discussing concerns their localizations in membranes. As noted on p. 528, when incubation times are short the reaction product is sometimes seen on the membranes and not in the spaces between adjacent membranes. It is, therefore, tempting to conclude that the enzymes are, in fact, situated in or on the membranes. But, as previously noted (23, 12), until more is known about the factors influencing precipitation of lead salts (particularly at the level of electron microscopy), this conclusion must remain provisional.

The observed acetylcholinesterase localizations are of considerable interest. Unequivocal demonstration of reaction product at the axoplasmic surface of myelinated fibers is relevant to the view deduced from biochemical data by Nachmansohn (19, 20) that the enzyme is present in the cell membrane and is related to the propagation of the nerve impulse (also see Koelle, reference 17). Fukuda and Koelle (9) and Taxi (41) have reported the presence of this enzyme in the cytoplasm of ganglion neurons, and they have emphasized that the distribution of reaction product corresponds with that of Nissl substance. Our present findings, together with earlier observations of Torack and Barnett (44) using thiolacetate as substrate in the presence of BW 62C47, indicate its localization in the endoplasmic reticulum. We have still to discover what relation, if any, exists between the enzyme in the

endoplasmic reticulum and that at the axoplasmic surface. Possibly the enzyme, synthesized at the ribosomes, is transported through the endoplasmic reticulum to and down the axon. Possibly relevant in this respect is the rapid accumulation of acetylcholinesterase activity in the crushed sciatic nerve proximal to the crushed region (22).

The question of artifact in nucleoside phosphatase preparations merits some comment. On p. 528, reasons are given for considering as diffusion artifacts the reaction product seen in myelinated fibers along the outer surfaces of the myelin and within vacuoles at the Schwann cell surfaces. We believe that the diffuse reaction product seen in the basement membranes of ganglion and nerve may also be artifact. Torack (43) has recently attributed light deposits of reaction product in "tubular profiles" (presumably endoplasmic reticulum; see 14) within the axoplasm of myelinated fibers in rat cerebrum (corpus callosum) to adenosine triphosphatase activity. The two electron micrographs illustrating these deposits are apparently from tissue incubated as blocks. In such blocks, artifacts due to limited penetration of reagents may be anticipated (reference 12; see especially p. 77 for a discussion of reaction product distributions reported in the glomerulus of kidney blocks). Furthermore, the level of reaction product is so low that experiments to rule out lead binding (see reference 14) would have been desirable. As seen above (pp. 526-527), myelinated fibers, in both dorsal root ganglia and sciatic nerve, give no evidence of hydrolyzing ATP or any of the other nucleoside phosphates, regardless of whether fixed or unfixed tissue is used and the incubation time is brief or long. We find the same result in myelinated fibers of rat cerebrum (corpus callosum) and optic nerve, studied by electron microscopy as well as light microscopy (25).

Although artifacts can, and do, occur, they can usually be readily recognized. Although the metabolic roles of the nucleoside phosphatases remain to be established, sections incubated for their presence are convenient preparations for demonstrating a variety of structures (24). Among the most striking are blood capillaries, perineurium cells of nerves (see reference 24 for a discussion of these cells), sheath cells of ganglia, and unmyelinated fibers. It is a simple matter to demonstrate the relative areas of unmyelinated (stained) and

myelinated (unstained) areas. In the rabbit thoracic vagus, in which most of the fibers are unmyelinated (8), virtually the entire nerve shows activity (Fig. 14 in reference 24), in contrast to the sciatic nerve of rat (Fig. 7), rabbit, and frog (Figs. 16 and 17 in reference 24) in which the ratio of myelinated to unmyelinated fibers is much greater.

These observations were presented at the 1964 International Summer School of Brain Research, in Amsterdam, Netherlands; an abbreviated account is in press (24).

This work was supported by research grants from the Public Health Service (CA-06576) and the Atomic Energy Commission (AT (30-1) 2786). The senior

author is a recipient of Public Health Service Research Career Program Award (5-K6-CA-14, 923) from the Cancer Institute.

Our thanks are due to Dr. Eric Holtzman for invaluable assistance with perfusion of nerve and ganglia, Mr. Jack Godrich for preparation of the photographs, Dr. Sidney Goldfischer and Dr. Alfred Angrist for critical reading of the manuscript, and Mrs. Sheila Schneider for secretarial assistance. We wish also to thank Dr. Morris J. Karnovsky, Harvard Medical School, for communicating the cholinesterase procedure used for electron microscopy prior to its publication, and Dr. John Smith, Montefiore Hospital, for providing us with methoxy acetyl- $\beta$ -methyl thiocholine iodide and the inhibitors RO20683 and BW62C47.

Received for publication 31 December 1965.

#### REFERENCES

1. BAKER, J. R., *Quart. J. Micr. Sc.*, 1944, **85**, 1.
2. BECKER, N. H., GOLDFISCHER, S., SHIN, W.-Y., and NOVIKOFF, A. B., *J. Biophysic. and Biochem. Cytol.*, 1960, **8**, 649.

---

FIGURE 20 Dorsal root ganglion, rat. Fixation: glutaraldehyde-cacodylate perfusion. Incubation: acetylcholine medium, 0°C, 145 min. Reaction product is seen in unmyelinated fibers (*U*), sheath cell surfaces (*S*) (see Fig. 27) and perikarya. In the perikarya, arrows indicate reaction product in endoplasmic reticulum and *N*, in nuclear envelope (see Fig. 28).  $\times 470$ .

FIGURE 21 Dorsal root ganglion, rat. Fixation: as in Fig. 19. Incubation: as in Fig. 19, but with  $2 \times 10^{-5}$  M 62C47 in the medium. Activity persists in unmyelinated fibers (*U*) and sheath cells (*S*), but is inhibited in the perikarya (*N*).  $\times 510$ .

FIGURE 22 Dorsal root ganglion, rat. Fixation: as in Fig. 19. Incubation, butyrylcholine medium, 0°C, 150 min. Reaction product is present in unmyelinated fibers (*U*) and sheath cells (*S*), but not in perikarya (*N*).  $\times 510$ .

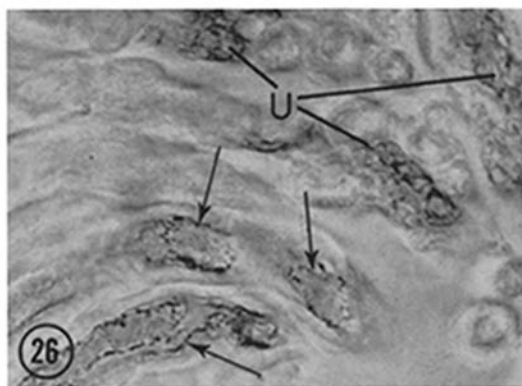
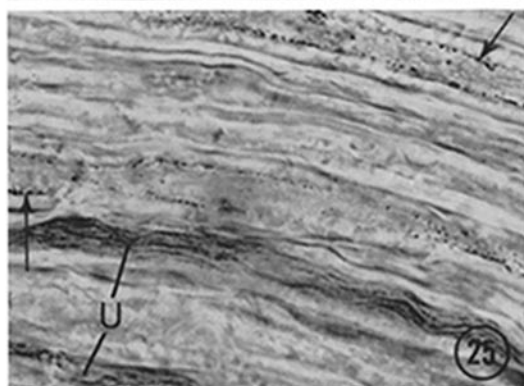
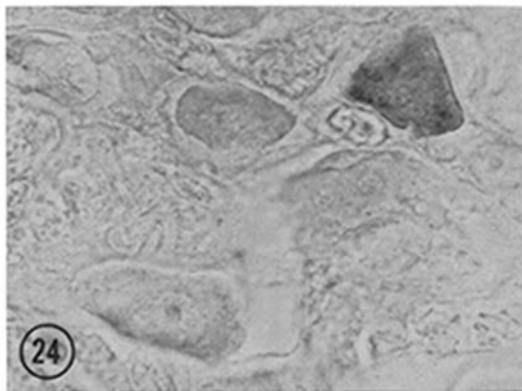
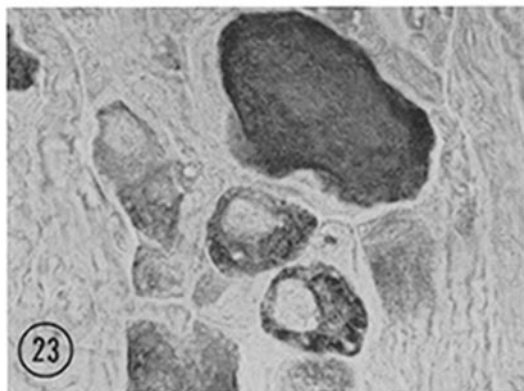
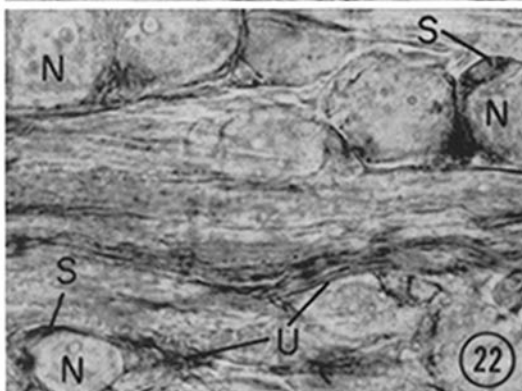
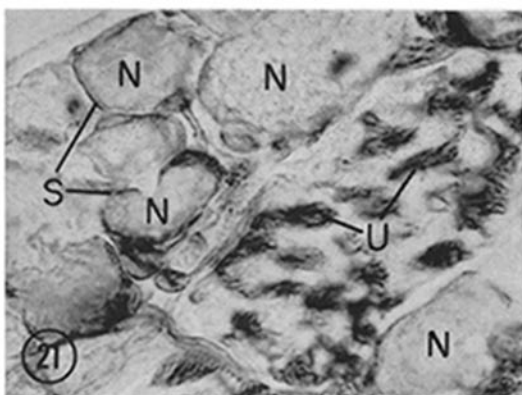
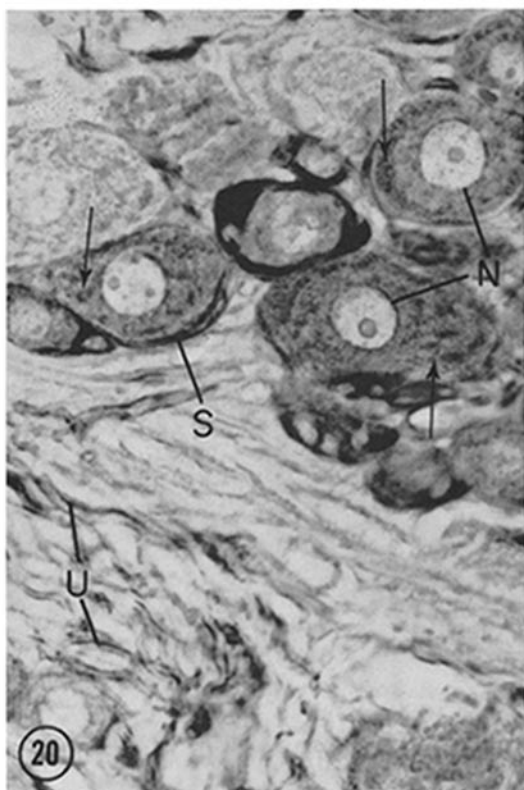
FIGURE 23 Dorsal root ganglion, frog. Fixation: 3% glutaraldehyde-cacodylate, immersion, 90 min. Incubation: acetylcholine medium, 25°C, 30 min. Although variable in amount, reaction product is seen in all neurons.  $\times 510$ .

FIGURE 24 Dorsal root ganglion, frog. Fixation: formaldehyde-calcium, immersion, 25 hr. Incubation: acetylcholine medium, 25°C, 2 hr. Most neurons show little or no reaction product; appreciable accumulation is seen only in the neuron at upper right. Compare with Fig. 23, in which the incubation time is only 30 min.  $\times 510$ .

FIGURE 25 Sciatic nerve, rat. Fixation: glutaraldehyde-cacodylate, perfusion. Incubation: acetylcholine medium, 0°C, 2 hr. Reaction product is seen in unmyelinated fibers (*U*) and at surface of axoplasm of myelinated fibers (arrows).  $\times 830$ .

FIGURE 26 Sciatic nerve, CF1 mouse. Fixation: 3% glutaraldehyde-cacodylate, immersion, 90 min. Incubation: acetylcholine medium, 0°C, 2 hr. Reaction product is seen in unmyelinated fibers (*U*) and at surface of axoplasm of myelinated fibers (arrows).  $\times 1,000$ .



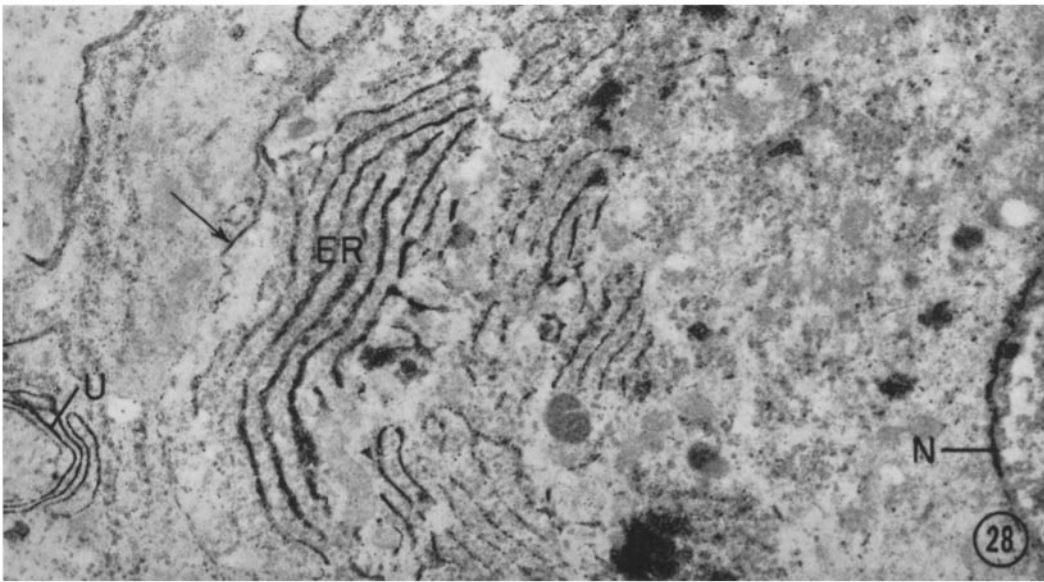
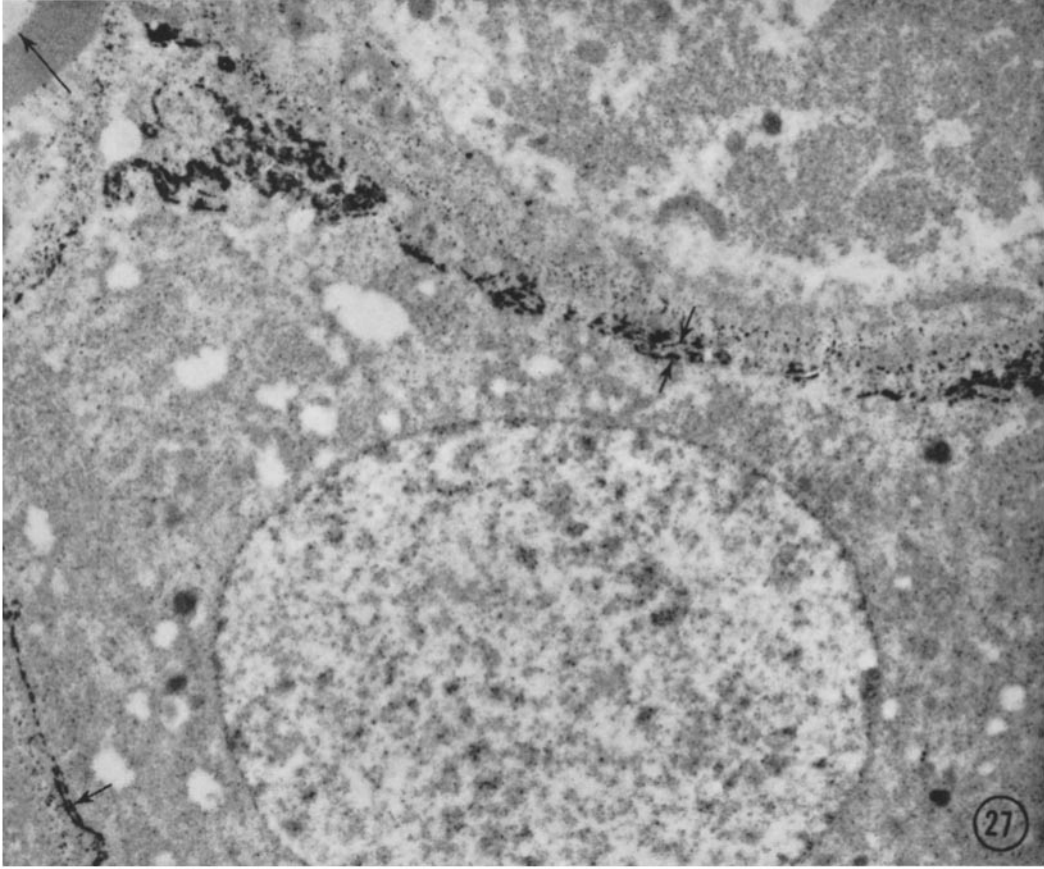


3. BONTING, S. L., SIMON, K. A., and HAWKINS, N. M., *Arch. Biochem. and Biophys.*, 1961, **95**, 416.
4. CAULFIELD, J. B., *J. Biophysic. and Biochem. Cytol.*, 1957, **3**, 827.
5. COLE, D. F., *Exp. Eye Research*, 1964, **3**, 72.
6. DUNHAM, E. T., and GLYNN, I. M., *J. Physiol.*, 1961, **156**, 274.
7. ERÄNKÖ, O., HÄRKÖNEN, M., KOKKO, A., and RÄISÄNEN, L., *J. Histochem. and Cytochem.*, 1964, **12**, 570.
8. EVANS, D. H. L., and MURRAY, J. G., *J. Anat.*, 1954, **88**, 320.
9. FUKUDA, T., and KOELLE, G. B., *J. Biophysic. and Biochem. Cytol.*, 1959, **5**, 433.
10. GLAUERT, A. M., and GLAUERT, R. H., *J. Biophysic. and Biochem. Cytol.*, 1958, **4**, 191.
11. GOLDFISCHER, S., *J. Histochem. and Cytochem.*, 1965, **13**, 520.
12. GOLDFISCHER, S., ESSNER, E., and NOVIKOFF, A. B., *J. Histochem. and Cytochem.*, 1964, **12**, 72.
13. HOKIN, L. E., and YODA, A., *Proc. Nat. Acad. Sc.*, 1964, **52**, 454.
14. HOLTZMAN, E., and NOVIKOFF, A. B., *J. Cell Biol.*, 1965, **27**, 651.
15. KARNOVSKY, M. J., *J. Cell Biol.*, 1964, **23**, 217.
16. KARNOVSKY, M. J., and ROOTS, L., *J. Histochem. and Cytochem.*, 1964, **12**, 219.
17. KOELLE, G. B., in *Handbuch der Experimentellen Pharmakologia Ergänzungswerk* (O. Eichler and A. Farah, editors), Berlin, Springer-Verlag, 1963, **15**, 189.
18. McCLURKEN, I. T., *J. Histochem. and Cytochem.*, 1964, **12**, 654.
19. NACHMANSOHN, D., *Chemical and Molecular Basis of Nerve Activity*, New York and London, Academic Press Inc., 1959.
20. NACHMANSOHN, D., *Handbuch der Experimentellen Pharmakologie Ergänzungswerk* (O. Eichler and A. Farah, editors), Berlin, Springer-Verlag, 1963, **15**, 701.
21. NOVIKOFF, A. B., *Circulation*, 1962, **26**, 1126.
22. NOVIKOFF, A. B., *Am. J. Path.*, 1964, **44**, 24a.
23. NOVIKOFF, A. B., in *Intracellular Membraneous Structure*, (S. Seno and E. V. Cowdry, editors), Okayama, Japan, Japan Society for Cell Biology, 1965, 277.
24. NOVIKOFF, A. B., Enzyme localization and ultrastructure of neurons, *Progr. Brain Research*, in press.
25. NOVIKOFF, A. B., Lysosomes in nerve cells, *Progr. Brain Research*, in press.
26. NOVIKOFF, A. B., and GOLDFISCHER, S., *Proc. Nat. Acad. Sc.*, 1961, **47**, 802.
27. NOVIKOFF, A. B., and MASEK, B., *J. Histochem. and Cytochem.*, 1958, **6**, 217.
28. NOVIKOFF, A. B., GOLDFISCHER, S., and ESSNER, E., *J. Histochem. and Cytochem.*, 1961, **9**, 459.
29. NOVIKOFF, A. B., SHIN, W.-Y., and DRUCKER, J., *J. Histochem. and Cytochem.*, 1960, **8**, 37.
30. NOVIKOFF, A. B., DRUCKER, J., SHIN, W.-Y., and GOLDFISCHER, S., *J. Histochem. and Cytochem.*, 1961, **9**, 434.
31. NOVIKOFF, A. B., ESSNER, E., GOLDFISCHER, S., and HEUS, M., *Symp. Internat. Soc. Cell Biol.*, 1962, **1**, 149.
32. OSTROWSKI, K., and BARNARD, E. A., *Exp. Cell Research*, 1961, **25**, 465.
33. OSTROWSKI, K., BARNARD, E. A., DARZYNKIEWICZ, Z., and RYMASZEWSKA, D., *Exp. Cell Research*, 1964, **36**, 43.
34. POST, R. L., MERRITT, C. R., KINSOLVING, C. R., and ALBRIGHT, C. D., *J. Biol. Chem.*, 1960, **235**, 1796.
35. REYNOLDS, E. S., *J. Cell Biol.*, 1963, **17**, 208.
36. ROSENBLUTH, J., *J. Cell Biol.*, 1962, **13**, 405.
37. ROSTGAARD, J., and BARNETT, R. J., *J. Ultrastruct. Research*, 1964, **11**, 193.

---

FIGURE 27 Dorsal root ganglion, rat. Incubation: frozen section, butyrylcholine medium, 0°C, 150 min. Thin section stained with uranyl acetate. Reaction product is seen at the interface between perikaryon and sheath cell (short arrows) but not within the perikaryon or at the surface of the axoplasm in the myelinated fiber (long arrow).  $\times 7,100$ .

FIGURE 28 Dorsal root ganglion, rat. Incubation: "chopper" section, acetylcholine medium, 0°C, 150 min. Thin section stained with uranyl acetate. Reaction product is seen in nuclear envelope (N), endoplasmic reticulum (ER), interface between perikaryon and sheath cell (arrow), and at the interfaces between Schwann cells and axoplasm and mesaxons of unmyelinated fibers (U). The unmyelinated fiber localizations are better visualized in Figs. 29 and 30; compare Figs. 10, 12, and 14, showing nucleoside phosphatase localizations in these fibers.  $\times 13,000$ .



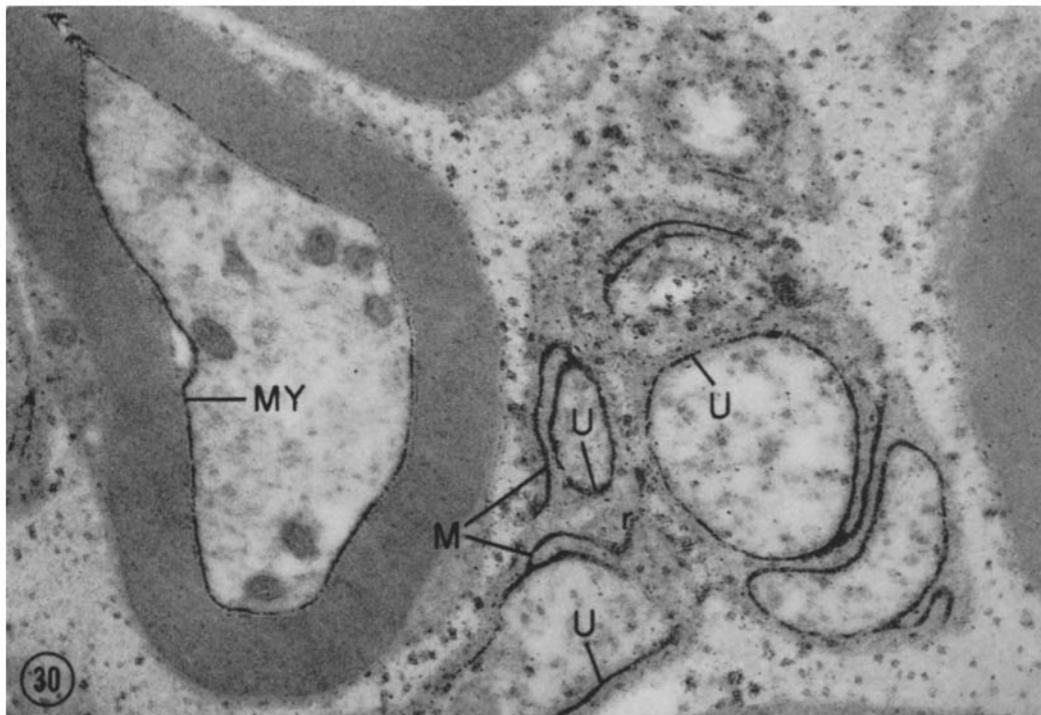


FIGURE 29 Dorsal root ganglion, rat. Incubation: "chopper" section, acetylcholine medium, 0°C, 150 min. Thin section stained with uranyl acetate. Reaction product is seen at the axoplasmic surfaces of myelinated fibers (MY) and the mesaxons (M) and axoplasm-Schwann cell interfaces of unmyelinated fibers (U).  $\times 9,400$ .

FIGURE 30 Dorsal root ganglion, rat. Incubation: "chopper" section, acetylcholine medium, 0°C, 150 min. Thin section not stained with uranyl acetate. Reaction product is seen at the axoplasmic surface of myelinated fibers (MY) and at the mesaxons (M) and interfaces between axoplasm and Schwann cells of unmyelinated fibers (U).  $\times 26,000$ .

38. SABATINI, D. D., BENSCH, K. G., and BARNETT, R. J., *J. Cell Biol.*, 1963, **17**, 19.
39. SKOU, J. C., *Biochim. et Biophysica Acta*, 1957, **23**, 394.
40. SMITH, R. E., and FARQUHAR, M., *Scient. Instr. News, RCA*, 1965, **10**, 13.
41. TAXI, J., *Bibl. Anat.*, 1961, **2**, 73.
42. TOOZE, J., *J. Cell Biol.*, 1965, **26**, 209.
43. TORACK, R. M., *J. Histochem. and Cytochem.*, 1965, **13**, 191.
44. TORACK, R. M., and BARNETT, R. J., *Exp. Neurol.*, 1962, **6**, 224.
45. WACHSTEIN, M., and MEISEL, E., *Am. J. Clin. Path.*, 1957, **27**, 13.
46. WATSON, M. L., *J. Biophysic. and Biochem. Cytol.*, 1958, **4**, 475.